Synthesis and anticancer cytotoxicity with structural context of an α-hydroxyphosphonate based compound library derived from substituted benzaldehydes

Zita Rádai[a], Tímea Windt[b], Veronika Nagy[b], András Füredi[b,c], Nóra Zsuzsa Kiss[a], Ivan Ranđelović[d,e], József Tóvári[d,e], György Keglevich[a], Gergely Szakács[b,c] and Szilárd Tóth[b]

[a] Department of Organic Chemistry and Technology, Budapest University of Technology and Economics, Budapest, Hungary.

[b] Institute of Enzymology, Research Centre for Natural Sciences, Hungarian Academy of Sciences, Budapest, Hungary. Correspondence to: toth.szilard.enzim@ttk.mta.hu and szakacs.gergely@ttk.mta.hu

[c] Institute of Cancer Research, Medical University Vienna, Vienna, Austria.

[d] National Institute of Oncology, Department of Experimental Pharmacology, Budapest, Hungary

[e] Kineto Lab ltd., Budapest, Hungary

ABSTRACT

We synthesized substituted benzaldehyde derived α-hydroxyphosphonates (αOHP), α-hydroxyphosphonic acids (αOHPA) and α-phosphinoyloxyphosphonates (αOPP) and characterized their cytotoxicity against a panel of cancer cell lines. A library containing 56 analogues was screened against Mes-Sa parental and Mes-Sa/Dx5 multidrug resistant uterine sarcoma cell lines, using a fluorescence-based cytotoxicity assay. The cytotoxicity screening revealed that dibenzyl-αOHPs and dimethyl-α-diphenyl-OPPs were the most active clusters, which encouraged us to synthesize further dibenzyl-α-diphenyl-OPP derivatives that elicited pronounced cell killing. Further structure-activity relationships showed the relevance of hydrophobicity and the position of substituents on the main benzene ring as determinants of toxicity. The most active analogs proved to be equally, or even more toxic to the multidrug resistant (MDR) cell line Mes-Sa/Dx5, suggesting these compounds may overcome P-glycoprotein mediated multidrug resistance by evading the drug transporter.

Footnotes

Electronic supplementary information (ESI) available: δ_P and MS value of the analogues; primary growth inhibition values; reaction time and yield of products.

1. Introduction

Organophosphonate derivatives, such as α-hydroxyphosphonates (αOHP), α-hydroxyphosphonic acids (αOHPA) and α-phosphinoyloxyphosphonates (αOPP) are a class of compounds of chemical and biological relevance. In synthetic chemistry, αOHPs are used in the synthesis of α-aminophosphonates, α-alkoxy-, or α-acyloxyphosphonates, ketophosphonates or α-halophosphonates.[1] In addition, several αOHPs, αOHPAs and αOPPs were found to be biologically active. For example, organic phosphonates were reported to possess moderate viral cysteine protease inhibitory,[2] antimicrobial or antifungal activities.[3-5] The αOPP SR-202 inhibits human peroxisome proliferator-activated receptor-γ (PPARγ), influencing insulin sensitivity and glucose consumption of cells.[6, 7] Studies have shown that organic phosphonates may influence cancer progression through the inhibition of farnesyl protein transferase (FPT)[8], which has emerged as a novel target for anti-cancer agents due to its role in the posttranslational modification of the Ras oncogene,[9] or purine nucleoside phosphorylase (PNP), as PNP inhibitors are potentially applicable in the management of certain hematologic malignancies.[10, 11]

However, to date, the direct anticancer activity of αOHP, αOHPA and αOPP analogues have not been systematically tested.[12]

In a recent study we identified cytotoxic αOHP analogues using the uterine sarcoma Mes-Sa cells.[13] Here our aim was to synthesize and characterize the cytotoxic profile of a diverse compound set, and to draw basic structure activity relationships against a panel of cell lines, including Mes-Sa/Dx5, the multidrug resistant (MDR) derivative of the Mes-Sa cell line.

2. Results and discussion

2.1. Synthesis and compilation of the chemical library

The derivatives were synthesized through the Pudovik reaction and subsequent modifications. Considering green chemical aspects, the reactions were performed either without solvent or in a minimal quantity of acetone, and the pure products were crystallized after reflux and adding a small amount of n-pentane[14] (Scheme 1, Scheme 2 and Scheme 3).

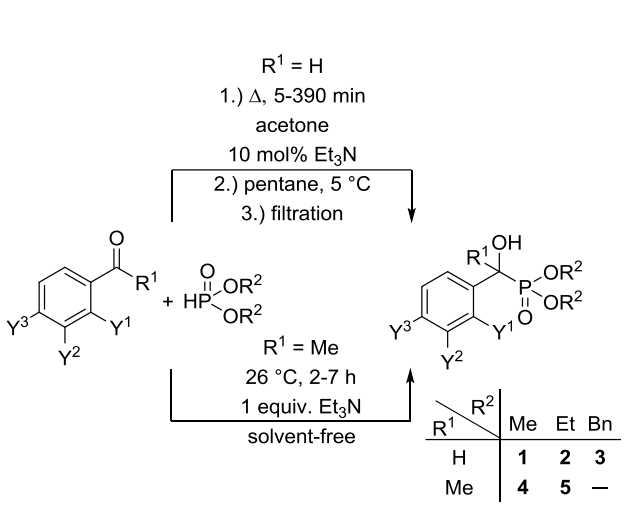

	R¹	R²	Y¹	Y²	Y³	Yield (%)
1a	H	Me	-	-	-	95
1b			Cl	-	-	93
1c			-	Cl	-	93
1d			-	-	Cl	90
1e			NO_2	-	-	95
1f			-	-	NO_2	95
1g			-	Me	-	92
1h			-	-	Me	89
1i			O-Me	-	-	68
1j			-	O-Me	-	98
1l			-	-	F	96
2a		Et	-	-	-	78
2b			Cl	-	-	80
2c			-	Cl	-	98
2d			-	-	Cl	79
2e			NO_2	-	-	89
2f			-	-	NO_2	88
3a		Bn	-	-	-	95
3b			Cl	-	-	93
3c			-	Cl	-	88
3d			-	-	Cl	95
3e			NO_2	-	-	91
3f			-	-	NO_2	99
3g			-	Me	-	88
3h			-	-	Me	94
3i			O-Me	-	-	96
4a	Me	Me	-	-	-	48
4f			-	-	NO_2	82
4k			F	-	-	56
4l			-	-	F	38
4m			-	Br	-	89
4n			-	-	Br	72
5f		Et	-	-	NO_2	65

Scheme 1. General scheme of the synthesis and the synthesized series of αOHPs (**1**, **2**, **3**, **4** and **5**). Dash signs in the table under Y1 – Y3 refer to hydrogen; Bn: benzyl.

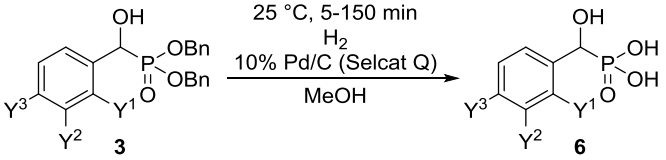

	Y¹	Y²	Y³	Yield (%)
6a	-	-	-	80
6b	Cl	-	-	85
6c	-	Cl	-	76
6d	-	-	Cl	88
6g	-	Me	-	77
6h	-	-	Me	90
6i	O-Me	-	-	72
6o	-	-	NH_2	50

Scheme 2. General scheme of the synthesis and the synthesized αOHPAs (**6**). Dash signs in the table under Y1 – Y3 refer to hydrogen; Bn: benzyl.

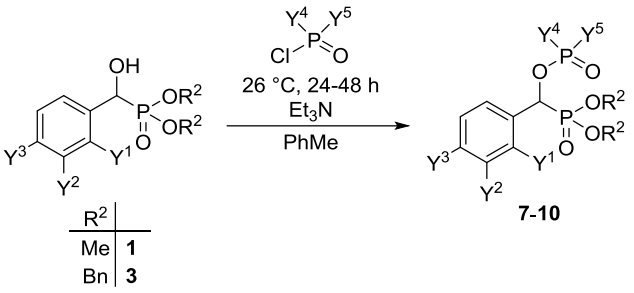

	R²	Y¹	Y²	Y³	Y⁴	Y⁵	Yield (%)
7a	Me	-	-	-	Ph	Ph	57
7d		-	-	Cl			61
7e		NO_2	-	-			79
7f		-	-	NO_2			70
7h		-	-	Me			49
8a		-	-	-			59
8d		-	-	Cl			54
8f		-	-	NO_2			72
8h		-	-	Me			46
9a		-	-	-			59
9d		-	-	Cl			51
9f		-	-	NO_2			80
9h		-	-	Me			50
10a	Bn	-	-	-	Ph	Ph	81
10c		-	Cl	-			57

Scheme 3. General scheme of the synthesis and the synthesized series of αOPPs (**7**, **8**, **9** and **10**). Dash signs in the table under Y1 – Y3 refer to hydrogen; Bn: benzyl; Ph: phenyl.

2.2. Primary screening of the phosphonate library

A library containing 56 derivatives of αOHPs, αOHPAs and αOPPs was screened against the Mes-Sa parental and Mes-Sa/Dx5 multidrug resistant uterine sarcoma cell lines, both engineered previously to express the mCherry fluorescent protein (Mes-Sa mCh and Mes-Sa/Dx5 mCh).[15] Primary cytotoxicity was defined as at least 50% growth inhibition compared to the untreated cells, and was determined

based on the fluorescence intensity of mCherry. At 20 µM, none of the analogues were effective, while at 200 µM, 11 entities (**3a**-**c**, **3e-i**, **7a**, **7d-e**, **7h**) were toxic to both Mes-Sa mCh and Mes-Sa/Dx5 mCh, and 3 additional compounds (**3d**, **4f**, **7f**) were selectively toxic to Mes-Sa/Dx5 mCh (Table S2).

2.3. Confirmation of dose-dependent cytotoxicity

Based on their primary cytotoxic effect, dibenzyl-αOHPs (**3a-i**) and dimethyl-α-diphenyl-OPPs (**7a**, **7d**-**f**, **7h**) were chosen for further investigations. As these two classes of analogues can be chemically 'combined', we designed and synthesized dibenzyl-α-diphenyl-OPP compounds (**10a**, **10c**) to see if we can produce analogues with increased cytotoxic potency.

We acquired dose-response curves and determined cytotoxicity as IC_{50} values against Mes-Sa mCh and Mes-Sa/Dx5 mCh cells. Against Mes-Sa mCh, **3a**-**i** exerted moderate toxicity (IC_{50} values ranging from 83 to 105 µM), except for the para-chloro (**3d**) and para-methyl (**3h**) substituted entities, which were remarkably less toxic with IC_{50} values exceeding 250 µM. Interestingly, multidrug resistant Mes-Sa/Dx5 mCh cells were more sensitive to these compounds (**3a**-**i**), with IC_{50} values in the range of 34 - 78 µM, and 126 µM for **3h**. Compounds **7a**, **7d**-**f** and **7h** were also only moderately toxic against the Mes-Sa mCh cell line (IC_{50} values between 98 - 270 µM) and against Mes-Sa/Dx5 mCh (35 - 221 µM). Remarkably, the newly synthesized analogues **10a** and **10c** showed increased toxicity with IC_{50} values around 10 µM against both Mes-Sa mCh and Mes-Sa/Dx5 mCh cells (Fig. 1A).

Since most compounds exerted significantly greater toxicity against the Mes-Sa/Dx5 mCh cell line than against Mes-Sa mCh, and since Mes-Sa/Dx5 mCh cells are multidrug resistant due to the overexpression of P-glycoprotein (P-gp), we checked if the paradoxical selective toxicity of the analogues were linked to the function of P-gp, as in the case of the so-called MDR-selective compounds.[15-18] However, the presence of the P-gp inhibitor tariquidar did not influence the selective toxicity of the compounds (Fig. 1B), suggesting that the observed collateral sensitivity was linked to other, cell line-specific factor(s) acquired by Mes-Sa/Dx5 cells during doxorubicin selection. On the other hand, no compounds were found to be effluxed by the transporter, thus the tested compounds can overcome this clinically important form of multidrug resistance. [19-21]

To test the broader potency of the analogues, we selected 3 further cell lines originating from tumor types known to show poor response in the clinics. We investigated the cytotoxicity against HT-29 rectosigmoid adenocarcinoma and HOP-62 lung adenocarcinoma cell lines, and against the MALME-3M metastatic melanoma cell line transfected with eGFP to allow detection of cell survival in a fluorescent protein-based assay. [22] In addition to 9 analogues of dibenzyl-α-OHPs (**3a-i**) we tested **7a**, **10a** and **10c**. We found that **10a** and **10c** were much more toxic to all 3 cell lines, than the other analogues (Table 1).

As previously was suggested, organic phosphonates may have an effect on the function of RAS proteins by inhibiting FTP which farnesylates RAS.[8] To test whether the compounds we synthesized are showing mutant KRAS-specific toxicity, we tested 4 cytotoxic compounds (**3c**, **7a**, **10a** and **10c**) on a parental (H838) and on a mutant KRAS expressing (H838-G12D) lung adenocarcinoma cell line. However, no specific hypersensitivity or resistance to the tested molecules was observed against the H838-G12D cells (Table 1). These results could be explained by several ways: (1) the used αOHPs do not inhibit FTP, (2) growth and survival of H838 cells do not rely on KRAS activity or (3) FTP inhibition is not sufficient, because geranylgeranylation might activate KRAS and suppresses the effect of FTP inhibition.[23] Nevertheless, the selected 4 compounds showed toxicity against both cell lines suggesting a more general effectivity toward cancer cells.

Table 1. IC_{50} values of compounds **3a-i**, **7a**, **10a** and **10c** against HT-29 and HOP-62 cell lines, measured by PrestoBlue viability reagent, against Malme-3M eGFP cell line measured by the fluorescent protein-based assay, and against H838 and H838-G12D cell lines measured by MTT assay. Numbers represent IC_{50} values and standard deviations (sd) calculated from the individual pIC_{50} values.

	HT-29	HOP-62	MALME-3M eGFP	H838	H838-G12D
	IC_{50} ± sd	IC_{50} ± sd	IC_{50} ± sd	IC_{50} ± sd	IC_{50} ± sd
3a	288.6 + 74.1 - 58.9	236.8 + 25.7 - 23.2	115.3 + 37.1 - 28.1		
3b	110.4 + 8.8 - 8.1	112.8 + 3.7 - 3.6	82.0 + 11.6 - 10.1		
3c	110.5 + 7.3 - 6.9	89.5 + 1.9 - 1.8	79.4 + 3.7 - 3.5	116.6 + 3.9 - 3.7	109.5 + 5.2 - 5.0
3d	>>500	173.4 + 55.4 - 42.0	151.5 + 50.4 - 37.8		
3e	116.1 + 16.7 - 14.6	97.8 + 18.5 - 15.6	76.5 + 8.4 - 7.6		
3f	129.7 + 16.5 - 14.6	104.9 + 5.3 - 5.0	89.5 + 10.9 - 9.7		
3g	117.6 + 10.3 - 9.4	95.3 + 7.5 - 7.0	84.4 + 12.7 - 11.1		
3h	>>500	>>500	215.4 + 79.8 - 58.2		
3i	154.7 + 9.6 - 9.0	110.9 + 11.8 - 10.6	88.3 + 3.7 - 3.5		
7a	337.1 + 40.4 - 45.8	301.8 + 27.7 - 30.4	214.2 + 26.4 - 30.1	226.0 + 0.5 - 0.5	180.1 + 1.3 - 1.3
10a	27.6 + 1.1 - 1.1	26.5 + 2.3 - 2.1	30.7 + 2.7 - 2.4	18.6 + 0.6 - 0.5	14.4 + 0.1 - 0.1
10c	24.5 + 4.4 - 3.7	15.1 + 5.3 - 3.9	13.4 + 0.1 - 0.1	14.4 + 0.3 - 0.3	13.7 + 0.6 - 0.6

2.4. Toxicity against the human non-cancerous cell line HFF

Cancer specific toxicity of representatives of our compound library (**3c**, **7a**, **10a** and **10c**) was probed against the human foreskin fibroblast (HFF) cell line. Based on the IC_{50} values (Table 2), we observed selectivity over tumor cells (note that HOP-62 and HT-29 cell lines were probed with the same viability reagent as HFF). The more pronounced vulnerability of cancer cells was not obvious, since in a study reporting the cytotoxicity of ß-formyl-α-hydroxyphosphonate derivatives, 2 out of 3 test compounds were more toxic to HFF as to the ID8 ovarian cancer cells.[24]

Table 2. IC_{50} values of compounds **3c**, **7a**, **10a** and **10c** against HFF, measured by PrestoBlue viability reagent. Numbers represent IC_{50} values and standard deviations (sd) calculated from the individual pIC_{50} values.

	HFF	
	IC_{50} ± sd	
3c	242.2	+ 23.4 - 25.9
7a	>>400	
10a	61.2	+ 1.6 - 1.6
10c	32.8	+ 3.4 - 3.7

2.5. Investigation of cell death

As apoptotic cells can be quickly cleared by macrophages, while cell debris derived from necrosis can cause inappropriate inflammation, apoptosis is the preferred cell death mechanism, when drug candidates are tested.[25, 26] To elucidate the mechanism of cytotoxicity of our analogues, we performed Annexin binding assays[27]. As shown in Fig. 2, treatment with either **3c** or **10c** induced apoptosis, and the proportion of late apoptotic/necrotic cells was increased remarkably after 48 h treatment.

2.6. Relationship of primary toxicity and lipophilicity

Growth inhibition at 200 µM (Table S2) shows correlation with the lipophilicity of the compounds (Fig. 3). With the exception of **4f** and **5f** (which had an approx. 50% inhibition against Mes-Sa/Dx5 mCh), compounds below a logP (partition coefficient) of 3 were not toxic. With a logP between 4-6, compounds were likely to be active. Furthermore, the most toxic analogues **10a** and **10c** have a logP of 9.3 and 8.8, respectively. Based on drug-like filters such as Lipinksi's rule of 5 and the Ghose filter, logP of drugs are preferred to be under 5 or between -0.4 and +5.6, respectively.[28, 29] One possibility of further drug development of **10a** and **10c** is to increase their hydrophilicity by introducing certain substituents, or/and design formulations that ensure their adequate bioavailability. As an example, Navitoclax, an anticancer Bcl-2 inhibitor that has a logP of 8.06 can be administered orally in a lipid solution.[30] Similarly, formulations of venetoclax[31] (logP: 6.76) and bexarothene[32] (logP: 6.94), which are also in use for cancer, play a key role.

2.7. Toxicity patterns

In general, αOHPAs (**6**), such as dimethyl- and diethyl-αOHPs (**1**, **2**, **4**, **5**) were not toxic, although an extra α-methyl-moiety improved toxicity (based on the activity of **4f** and **5f** against Mes-Sa/Dx5 mCh). However, when dibenzyl-αOHPs were investigated (**3**), toxicity increased remarkably. This increase in activity was observed also when dimethyl- and dibenzyl- αOPPs (**7** and **10**) were compared. We found relevant features linked to the position of the substituents on the main benzene ring. When the substituent was chlorine, the toxicity increased in the direction of para < ortho ≤ meta positions

throughout the cell panel. In the case of the NO_2 group, the ortho-position was also beneficial as compared to the para-position, especially in the case of Mes-Sa/Dx5 mCh. Moreover, the meta-position was much more beneficial than the para-position when methyl substitutions were present. This pattern indicates that substituents in the meta-position were preferred among **3a-i** (Table 3). Our results provide the first detailed insights of the structure-anticancer activity relationship of the said organophosphonates, as earlier studies on salicylaldehide derived αOHPs[12] or on ß-formyl-αOHPs[24] identified only a few compounds with cytotoxic potential, without relevant SAR observations.

Table 3. Relative toxicity of **3a-i**. IC_{50} values were normalized to the IC_{50} of the unsubstituted benzene ring containing compound (**3a**). Substituents on the benzene ring: o (ortho) refers to Y1; m (meta) refers to Y2 and p (para) to Y3 (Scheme 1). Mean rel. IC_{50} is the average of the individual relative IC_{50} values.

	substituent	Mes-Sa	Mes-Sa/Dx5	Malme-3M	HT-29	HOP-62	Mean rel.
	(Y1-Y2-Y3)	mCh	mCh	eGFP			IC_{50}
3a	H	1	1	1	1	1	1
3b	o-Cl	0.88	0.78	0.69	0.37	0.47	0.64
3c	m-Cl	0.89	0.54	0.66	0.37	0.38	0.57
3d	p-Cl	2.86	1.02	1.31	1.69	0.76	1.53
3e	o-NO_2	0.90	0.45	0.64	0.40	0.42	0.56
3f	p-NO_2	1.02	0.87	0.75	0.44	0.44	0.70
3g	m-Me	1.11	0.99	0.71	0.40	0.40	0.72
3h	p-Me	2.87	1.70	1.88	1.69	2.10	2.05
3i	o-O-Me	0.89	0.97	0.74	0.52	0.47	0.72

3. Conclusions

By synthesizing and testing a library of αOHPs, αOHPAs and αOPPs, we identified potent anticancer agents inducing apoptosis in several cell lines of different origin. The relation between growth inhibition and hydrophobicity (logP) was revealed and quantified, which can be exploited as an in silico pre-screening step in future studies. Based on the IC_{50} values, we observed the increased toxicity of dibenzyl-αOHPs (**3**) and dibenzyl-αOPPs (**10**) compared to the other analogues, and found that the most beneficial position for a substituent on the main benzene ring was the meta-position. These results are so far the most detailed SAR observations pertaining to αOHPs, αOHPAs and αOPPs. We also noticed the collateral sensitivity of the multidrug resistant Mes-Sa/Dx5 mCh cell line against most of the tested analogues. Although this hypersensitivity was independent from the function of P-glycoprotein, the results show that the tested analogues can overcome multidrug resistance by evading the transporter.

4. Experimental

*General procedure for the synthesis of α-hydroxyphosphonates **1**, **2** and **3***

A mixture of 11.0 mmol of aromatic aldehyde (benzaldehyde: 1.2 g, 2-chlorobenzaldehyde: 1.5 g, 3-chlorobenzaldehyde: 1.5 g, 4-chlorobenzaldehyde: 1.5 g, 2-nitrobenzaldehyde: 1.7 g, 4-nitrobenzaldehyde: 1.7 g, 3-methylbenzaldehyde: 1.3 g, 4-methylbenzaldehyde: 1.3 g, 2-methoxybenzaldehyde: 1.5 g, 3-methoxybenzaldehyde: 1.5 g, 4-fluorobenzaldehyde: 1.4 g), 11.0 mmol of dialkyl phosphite (dimethyl phosphite: 1.1 mL, diethyl phosphite: 1.4 mL and dibenzyl phosphite: 2.4 mL) and 1.10 mmol (150 µl) of triethylamine was stirred in 1 mL of acetone at reflux.

After 5–390 min, 6 mL of pentane was added to the reaction mixture. On cooling, the product crystallized from the reaction mixture. Filtration afforded products **1**, **2** and **3** in a purity of > 99%.

*General procedure for the synthesis of α-hydroxyphosphonates **4** and **5***

A mixture of 11.0 mmol of aromatic ketone (acetophenone: 1.3 g, 2-fluoroacetophenone: 1.5 g, 4-fluoroacetophenone: 1.5 g, 3-bromoacetophenone: 2.2 g, 4-bromoacetophenone: 2.2 g, 4-nitroacetophenone: 1.8 g), 11.0 mmol of dialkyl phosphite (dimethyl phosphite: 1.1 mL or diethyl phosphite: 1.4 mL) and 11.0 mmol (1.5 mL) of triethylamine was stirred at 25 °C for 2–7 h. Completion of the reaction was indicated by the crystallization of the product from the reaction mixture. The reaction mixture was cooled to 5 °C. After the crystallization was complete, the white crystals were filtered off and were washed with 2 mL of hexane to afford **4a**, **4f**, **4k**, **4l**, **4m**, **4n** and **5f** in yields of 38–89%.

*General procedure for the synthesis of α-hydroxyphosphonic acids **6***

4.1 mmol of α-hydroxyphosphonate (**3a**: 1.5 g, **3b**: 1.7 g, **3c**: 1.7 g, **3d**: 1.7 g, **3f**: 1.7 g, **3g**: 1.6 g, **3h**: 1.6 g, **3i**: 1.6 g) was hydrogenated in the presence of 10% Pd/C (Selcat Q) (0.08–0.09 g, the catalyst/substrate ratio was 0.05 g/g) in 30 mL of methanol in a 80-mL stainless steel autoclave equipped with a magnetic stirrer (stirring speed = 1100 rpm). The hydrogenations took place at 10 bar and 25 °C in 5–150 minutes. Then, the catalyst was filtered off, and activated carbon (0.15–0.17 g) was added to the solution. After 1 h of stirring, the absorbent was filtered off, and the organic solvent was evaporated. 5 mL of CH_2Cl_2 was added to the crude product and stirred for 15 min at reflux. After filtration, α-hydroxyphosphonic acids were obtained in yields of 50–90%.

*General procedure for the synthesis of α-phosphinoyloxyphosphonates **7, 8, 9**, and **10***

A mixture of 1.0 mmol of α-hydroxyphosphonate (**1a**: 0.22 g, **1d**: 0.25 g, **1e**: 0.26 g, **1f**: 0.26 g , **1h**: 0.23 g, **3a**: 0.37 g, **3c**: 0.40 g), 5 mL of toluene, 1.2 mmol (0.17 mL) of triethylamine and 1.1 mmol of phosphinic chloride (diphenylphosphinic chloride: 0.21 mL, 1-chloro-3-methyl-3-phospholene-1-oxide: 0.17 g or 1-chloro-3,4-dimethyl-3-phospholene-1-oxide: 0.18 g) was stirred at 25 °C for 24-48 h under N_2 atmosphere. The precipitated triethylamine hydrochloride salt was filtered off, and the volatile compounds were removed under vacuum. The purification of the crude product with column chromatography on silica gel, using acetone:dichloromethane = 2:1 as the eluent afforded the corresponding α-phospinoyloxyphosphonates (**7**, **8**, **9** and **10**).

The identity of the analogues that were known from the literature were validated by the δ_P and MS values (Table S1).

7e. Yield: 79% ^{31}P NMR ($CDCl_3$) δ 17.0 (d, ^3J = 26.9, P(O)$(OCH_3)_2$), 34.6 (d, ^3J = 27.0, P(O)Ph_2); ^{13}C NMR ($CDCl_3$) δ 53.8 (d, ^2J = 6.7, OCH_3), 54.3 (d, ^2J = 7.0, OCH_3), 66.1 (dd, ^1J = 170.5, ^2J = 5.9, PCH), 124.9 (d, ^4J = 2.1, C_3), 128.4 (d, ^3J = 13.5, $C_{3'}$), 128.6 (d, ^3J = 13.4, $C_{3'}$), 129.2 (d, ^5J = 2.7, C_4), 133.4 (d, ^4J = 2.8, C_5), 130.0 (d, ^3J = 4.9, C_6) overlapped by 130.0 (C_1), 131.5 (d, ^1J = 146.8, $C_{1'}$), 131.6 (d, ^2J = 10.5, $C_{2'}$), 131.90 (d, ^1J = 130.1, $C_{1'}$), 131.93 (d, ^2J = 10.5, $C_{2'}$), 132.5 (d, ^4J = 2.9, $C_{4'}$), 132.8 (d, ^4J = 3.1, $C_{4'}$), 147.0 (d, ^3J = 5.3, C_2); ^{1}H NMR ($CDCl_3$) δ 3.62 (d, $^3J_{P,H}$ = 10.8, 3H, OCH_3), 3.75 (d, $^3J_{P,H}$ = 10.8, 3H, OCH_3), 6.80 (dd, $^{2,3}J_{P,H}$ = 11.1, 15.5, 1H, PCH), 7.31-7.74 (m, 10H, Ar), 7.88-8.03 (m, 4H, Ar).

10a. Yield: 81% ^{31}P NMR ($CDCl_3$) δ 18.1 (d, ^3J = 28.0, P(O)$(OBn)_2$), 35.0 (d, ^3J = 28.0, P(O)Ph_2); ^{13}C NMR ($CDCl_3$) δ 68.5 (d, ^2J = 6.9, CH_2), 68.6 (d, ^2J = 7.2, CH_2), 72.2 (dd, ^1J = 173.1, ^2J = 7.1, PCH), 127.2 (d, ^3J = 6.0, C_2), 127.8-128.6 (m, C_4, $C_{3'}$, $C_{2''}$, $C_{3''}$, $C_{4''}$), 128.9 (d, ^4J = 2.8, C_3), 130.89 (d, ^1J = 138.2, $C_{1'}$), 130.97 (d, ^1J = 134.0, $C_{1'}$), 131.7 (d, ^2J = 10.5, $C_{2'}$), 131.8 (d, ^2J = 10.6, $C_{2'}$), 132.1 (d, ^4J = 3.0, $C_{4'}$), 132.4 (d, ^4J = 2.9,

$C_{4'}$), 133.4 (t, ^{2}J = 1.3, ^{3}J = 1.3, C_1), 135.8 (d, ^{3}J = 6.0, $C_{1''}$), 136.0 (d, ^{3}J = 5.8, $C_{1''}$); ^{1}H NMR ($CDCl_3$) δ 4.67-5.10 (m, 4H, 2xCH_2), 5.75 (dd, $^{2,3}J_{P,H}$ = 10.8, 13.1, 1H, PCH), 7.03-7.90 (m, 25H, Ar).

10c. Yield: 57% ^{31}P NMR ($CDCl_3$) δ 17.6 (d, ^{3}J = 28.0, P(O)$(OBn)_2$), 35.5 (d, ^{3}J = 28.2, P(O)Ph_2); ^{13}C NMR ($CDCl_3$) δ 68.6 (d, ^{2}J = 6,8, CH_2), 68.8 (d, ^{2}J = 7.3, CH_2), 71.4 (dd, ^{1}J = 173.2, ^{2}J = 6.5, PCH), 126.5 (d, ^{3}J = 5.9, C_6), 127.9-128.7 (m, $C_{3'}$, $C_{2''}$, $C_{3''}$, $C_{4''}$) overlapped by 128.4 (d, ^{3}J = 6.1, C_2) 129.0 (d, ^{5}J = 2.7, C_4), 129.5 (d, ^{4}J = 1.9, C_5), 130.5 (d, ^{1}J = 137.8, $C_{1'}$), 130.7 (d, ^{1}J = 134.5, $C_{1'}$), 131.7 (d, ^{2}J = 10.6, $C_{2'}$), 131.8 (d, ^{2}J = 10.6, $C_{2'}$), 132.3 (d, ^{4}J = 3.0, $C_{4'}$), 132.5 (d, ^{4}J = 2.9, $C_{4'}$), 134.1 (d, ^{4}J = 2.3, C_3), 135.4 (t, ^{2}J = 1.4, ^{3}J = 1.4, C_1), 135.6 (d, ^{3}J = 6.1, $C_{1''}$), 135.8 (d, ^{3}J = 5.5, $C_{1''}$); ^{1}H NMR ($CDCl_3$) δ 4.76-5.05 (m, 4H, 2xCH_2), 6.80 (dd, $^{2,3}J_{P,H}$ = 10.3, 11.1, 1H, PCH), 7.07-7.89 (m, 24H, Ar).

4.1. Cell lines and culture conditions

To assess anticancer cytotoxicity, we used the HOP-62 lung adenocarcinoma, HT-29 rectosigmoid adenocarcinoma, Malme-3M melanoma and Mes-Sa and the multidrug resistant Mes-Sa/Dx5 uterine sarcoma cell lines, and in addition H838 and KRAS mutant H838-G12D lung adenocarcinoma cell lines. The uterine sarcoma lines and the human foreskin fibroblast (HFF) cells were obtained from ATCC, and were maintained in DMEM. H838 cells were from Horizon Discovery Group plc., while the other lines were purchased from the NCI DTP, and were cultivated in RPMI. Media were supplemented with 10 % FBS, 5 mmol/L glutamine, and 50 unit/mL penicillin and streptomycin (ThermoFisher), except for HFF, where we used a 20 % FBS containing medium.

4.2. Fluorescent protein transfection.

Mes-Sa and Mes-Sa/Dx5 cell lines were transfected with the fluorescent protein mCherry (mCh), and were already utilized in other studies.[13, 15, 22] Establishment of the Malme-M3 eGFP was not described earlier, but it was created with the same method. Briefly, the Malme-M3 cell line was transduced with the fluorescent protein expressing lentiviral supernatants produced with pRRL-EF1-eGFP expression plasmid. After the transduction, cell lines were sorted by flow cytometry based on fluorescent intensity.

4.3. Cytotoxicity assays

Cells were seeded on 384 well plates 1 day prior to drug addition at a 2500 cells/well density in every scenario but the H838 lines, where 5000 cells were seeded on 96 well plates. In the primary screening, we assessed the cytotoxicity against Mes-Sa mCh and Mes-Sa/Dx5 mCh cell lines in 20 µM and in 200 µM concentrations. Drug treatment took 96 h, then the fluorescent intensity of mCherry (ex/em: 585/610 nm) was detected with an EnSpire multimode plate reader (Perkin Elmer). In the following step, cells were treated with the serial dilution of the drugs showing activity in the primary screen, and IC_{50} values were acquired after 144 h incubation time. Dose-response curves for **3a-i**, **7a**, **10a** and **10c** were obtained against 3 additional cell lines to prove general anticancer toxicity of the selected compounds. Cytotoxicity against Malme-M3 eGFP was assessed via the detection of eGFP fluorescence (ex/em: 485/510 nm) after 144 h incubation, while the IC_{50} values against HOP-62 and HT-29 were calculated from the detection of PrestoBlue viability reagent (Thermo Fisher) conversion at ex/em of 555/585 nm wavelengths, 72 h post drug addition. Against compounds **3c**, **7a**, **10a** and **10c**, the viability of H838 lines were determined based on MTT assay, and based on PrestoBlue assay against HFF.

4.4. Cell death assessment

Annexin V/propidium iodide (PI) based apoptosis quantification was performed by using the Annexin V, FITC Apoptosis Detection Kit (Dojindo Molecular Technologies) according to the protocol provided by the manufacturer. Briefly, 1.5x10^5 HOP-62 cells were seeded on 12 well plates, treated with the

given drug at IC_{50} concentrations for 24 and 48 hours. Cells in the supernatant were collected and admixed with the cells that were detached with trypsin. Cells were stained for 15 minutes at room temperature in dark with 5 µl Annexin V and 5µl PI solution in a 10-fold diluted Annexin V binding buffer. Samples were analyzed by Attune NxT Flow Cytometer (Thermo Fisher Scientific).

Conflict of interest

There are no conflicts to declare.

Acknowledgements

The transfection of Malme-M3 cell line with the pRRL-EF1-eGFP expression plasmid was carried out by Nóra Kucsma (Institute of Enzymology, RCNS, HAS, Budapest, Hungary).

This work was supported by a Momentum grant of the Hungarian Academy of Sciences. Support of grant BME FIKP-BIO by Ministry of Human Capacities of Hungary (EMMI) is kindly acknowledged. The project was sponsored by the National Research Development and Innovation Fund (K119202). Z. Rádai was supported by the ÚNKP-18-3-IV-BME-265 New National Excellence Program of the Ministry of Human Capacities, and N.Z. Kiss was supported by the János Bolyai Research Scholarship of the Hungarian Academy of Sciences (BO/00130/19/7). J. Tóvári and I. Ranđelović were supported by the National Research, Development and Innovation Office, NVKP_16-1-2016-0020.

References

1. Z. Rádai and G. Keglevich, *Molecules*, 2018, **23**, 1493.
2. A. M. Prior, Y. Kim, S. Weerasekara, M. Moroze, K. R. Alliston, R. A. Uy, W. C. Groutas, K. O. Chang and D. H. Hua, *Bioorg Med Chem Lett*, 2013, **23**, 6317-6320.
3. A. H. Kategaonkar, R. U. Pokalwar, S. S. Sonar, V. U. Gawali, B. B. Shingate and M. S. Shingare, *Eur J Med Chem*, 2010, **45**, 1128-1132.
4. N. S. Patil, G. B. Deshmukh, S. V. Patil, A. D. Bholay and N. D. Gaikwad, *Eur J Med Chem*, 2014, **83**, 490-497.
5. R. U. Pokalwar, R. V. Hangarge, P. V. Maske and M. S. Shingare, *Arkivoc*, 2006, **11**, 196-204.
6. F. M. da Silva, J. C. dos Santos, J. L. Campos, A. C. Mafud, I. Polikarpov, A. C. Figueira and A. S. Nascimento, *Bioorg Med Chem Lett*, 2013, **23**, 5795-5802.
7. H. S. Wu, J. H. Yu, Y. Y. Li, Y. S. Yang, Q. J. He, Y. J. Lou and R. Y. Ji, *Acta Pharmacol Sin*, 2007, **28**, 417-422.
8. D. L. Pompliano, E. Rands, M. D. Schaber, S. D. Mosser, N. J. Anthony and J. B. Gibbs, *Biochemistry*, 1992, **31**, 3800-3807.
9. S. Bagchi, P. Rathee, V. Jayaprakash and S. Banerjee, *Mini Rev Med Chem*, 2018, **18**, 1611-1623.
10. A. Al-Kali, V. Gandhi, M. Ayoubi, M. Keating and F. Ravandi, *Future Oncol*, 2010, **6**, 1211-1217.
11. T. Yokomatsu, H. Abe, M. Sato, K. Suemune, T. Kihara, S. Soeda, H. Shimeno and S. Shibuya, *Bioorg Med Chem*, 1998, **6**, 2495-2505.
12. R. M. N. Kalla, H. R. Lee, J. Cao, J.-W. Yoo and I. Kim, *New Journal of Chemistry*, 2015, **39**, 3916-3922.
13. Z. Rádai, P. Szeles, N. Z. Kiss, L. Hegedűs, T. Windt, V. Nagy and G. Keglevich, *Heteroatom Chemistry*, 2018, **29**, e21436.
14. G. Keglevich, Z. Rádai and N. Z. Kiss, *Green Process Synth*, 2017, **6**, 197-201.
15. V. F. S. Pape, S. Tóth, A. Füredi, K. Szebényi, A. Lovrics, P. Szabó, M. Wiese and G. Szakács, *Eur J Med Chem*, 2016, **117**, 335-354.

16. G. Szakacs, J. P. Annereau, S. Lababidi, U. Shankavaram, A. Arciello, K. J. Bussey, W. Reinhold, Y. Guo, G. D. Kruh, M. Reimers, J. N. Weinstein and M. M. Gottesman, *Cancer Cell*, 2004, **6**, 129-137.
17. D. Turk, M. D. Hall, B. F. Chu, J. A. Ludwig, H. M. Fales, M. M. Gottesman and G. Szakacs, *Cancer Res*, 2009, **69**, 8293-8301.
18. A. Furedi, S. Toth, K. Szebenyi, V. F. Pape, D. Turk, N. Kucsma, L. Cervenak, J. Tovari and G. Szakacs, *Mol Cancer Ther*, 2017, **16**, 45-56.
19. A. Furedi, K. Szebenyi, S. Toth, M. Cserepes, L. Hamori, V. Nagy, E. Karai, P. Vajdovich, T. Imre, P. Szabo, D. Szuts, J. Tovari and G. Szakacs, *J Control Release*, 2017, **261**, 287-296.
20. G. Szakacs, J. K. Paterson, J. A. Ludwig, C. Booth-Genthe and M. M. Gottesman, *Nat Rev Drug Discov*, 2006, **5**, 219-234.
21. L. J. Goldstein, H. Galski, A. Fojo, M. Willingham, S. L. Lai, A. Gazdar, R. Pirker, A. Green, W. Crist, G. M. Brodeur and et al., *J Natl Cancer Inst*, 1989, **81**, 116-124.
22. T. Windt, S. Tóth, I. Patik, J. Sessler, N. Kucsma, Á. Szepesi, B. Zdrazil, C. Özvegy-Laczka and G. Szakács, *Archives of Toxicology*, 2019, DOI: 10.1007/s00204-019-02417-6.
23. D. B. Whyte, P. Kirschmeier, T. N. Hockenberry, I. Nunez-Oliva, L. James, J. J. Catino, W. R. Bishop and J. K. Pai, *J Biol Chem*, 1997, **272**, 14459-14464.
24. S. Perera, V. K. Naganaboina, L. Wang, B. Zhang, Q. Guo, L. Rout and C.-G. Zhao, 2011, **353**, 1729-1734.
25. S. Gordon and A. Pluddemann, *Front Immunol*, 2018, **9**, 127.
26. S. Nagata, *Annu Rev Immunol*, 2018, **36**, 489-517.
27. S. J. Martin, C. P. Reutelingsperger, A. J. McGahon, J. A. Rader, R. C. van Schie, D. M. LaFace and D. R. Green, *J Exp Med*, 1995, **182**, 1545-1556.
28. C. A. Lipinski, F. Lombardo, B. W. Dominy and P. J. Feeney, *Adv Drug Deliv Rev*, 2001, **46**, 3-26.
29. A. K. Ghose, V. N. Viswanadhan and J. J. Wendoloski, *Journal of Combinatorial Chemistry*, 1999, **1**, 55-68.
30. J. Yang, H. Xiong, A. Krivoshik, K. Holen, R. Pradhan, Y.-L. Chiu, A. Nada, A. Tolcher, W. Awni and R. Humerickhouse, 2011, **71**, 1300-1300.
31. A. E. Place, K. Goldsmith, J. P. Bourquin, M. L. Loh, L. Gore, D. A. Morgenstern, Y. Sanzgiri, D. Hoffman, Y. Zhou, J. A. Ross, B. Prine, M. Shebley, M. McNamee, T. Farazi, S. Y. Kim, M. Verdugo, L. Lash-Fleming, C. M. Zwaan and J. Vormoor, *Future Oncol*, 2018, **14**, 2115-2129.
32. H. M. Prince, C. McCormack, G. Ryan, C. Baker, H. Rotstein, J. Davison and R. Yocum, *Australas J Dermatol*, 2001, **42**, 91-97.

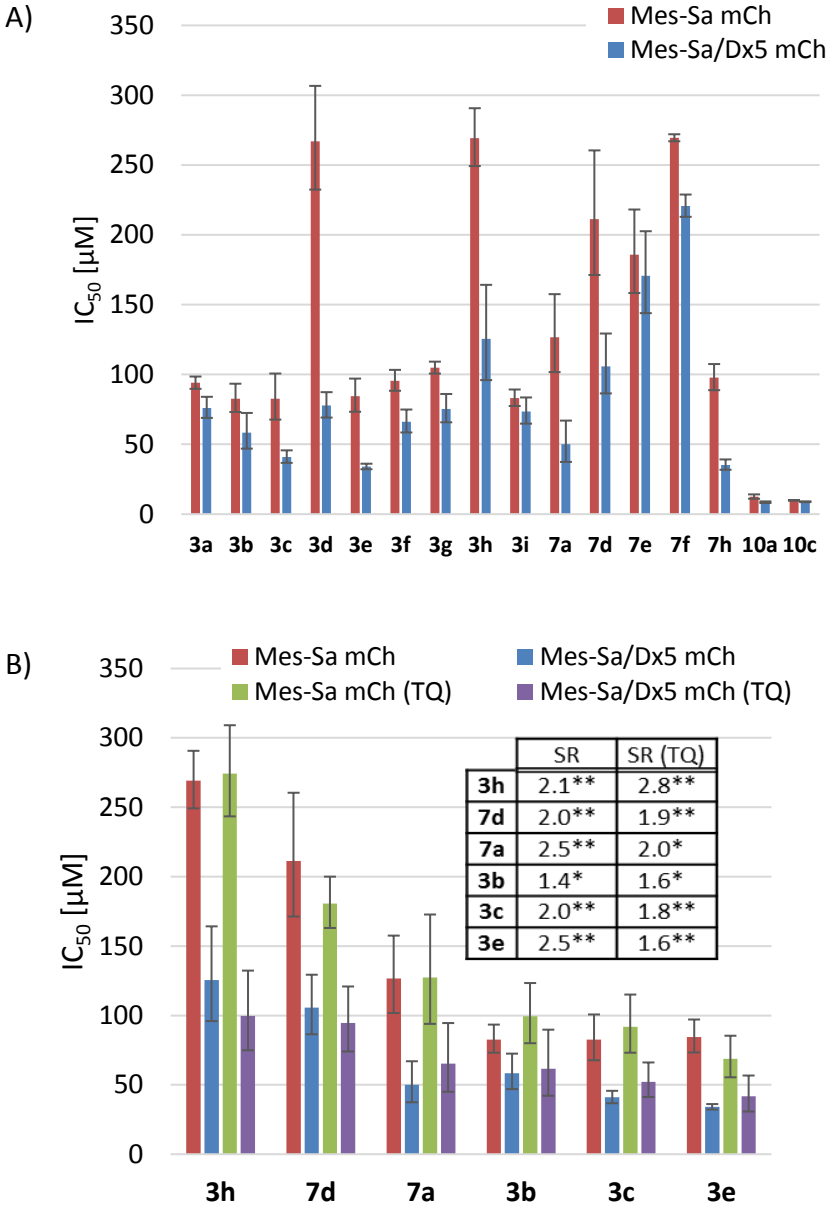

Figure 1. (A) IC_{50} values of compounds **3**, **7** and **10** against Mes-Sa mCh (red) and Mes-Sa/Dx5 mCh (blue) cell lines. Results of compounds **3** against Mes-Sa mCh were taken from our previous study.[13] (B) Cytotoxicity and selectivity ratio (SR = IC_{50} Mes-Sa mCh/IC_{50} Mes-Sa/Dx5 mCh) of compounds **3b**-**c**, **3e**, **3h**, **7a** and **7d**. IC_{50} values, standard deviations and significance (*, $P < 0.05$; **, $P < 0.01$) were calculated from the individual pIC_{50}s. TQ refers to the P-glycoprotein inhibitor tariquidar (0.4 µM).

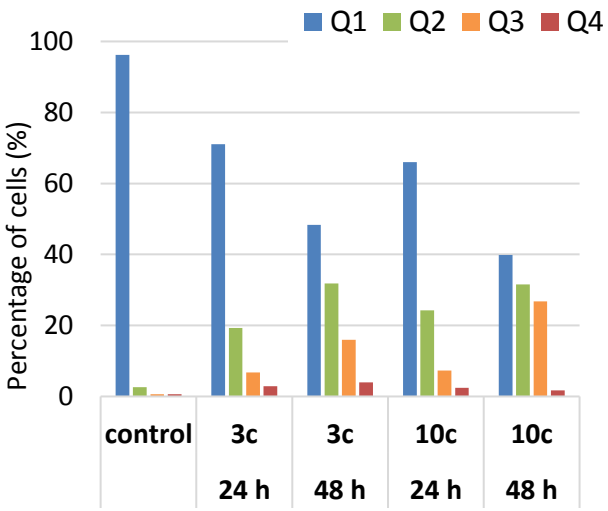

Figure 2. Induction of apoptosis of HOP-62 cells by **3c** or **10c**. The four quadrants indicate viable cells (Q1); only Annexin V positive cells (apoptosis, Q2); Annexin V and propidium-iodide positive cells (late apoptosis/necrosis, Q3); and only propidium-iodide positive cells (Q4).

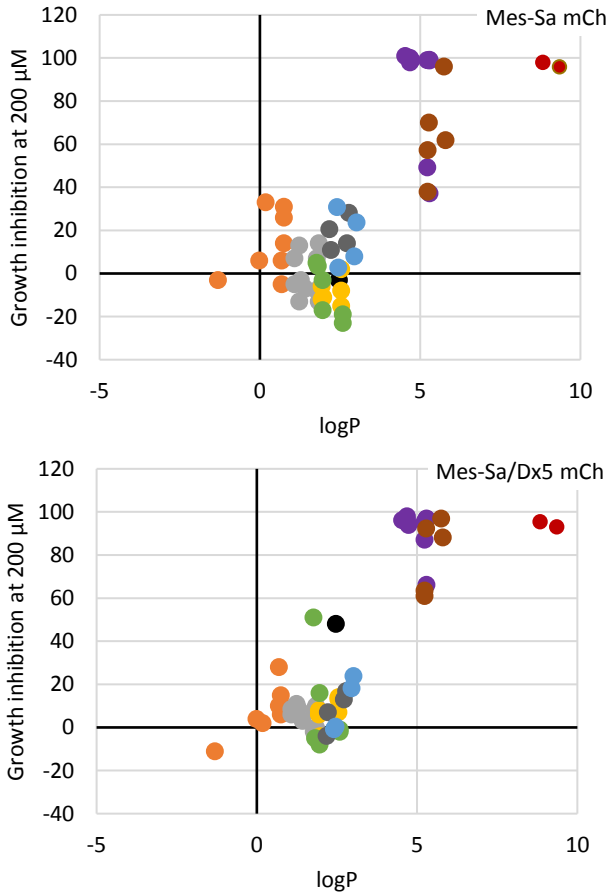

Figure 3. Growth inhibition of compounds at 200 µM after 96 h drug incubation as the function of logP. Compound groups from Scheme 1, 2 and 3 are presented with different colors, **1**: light grey, **2**: yellow; **3**: purple; **4**: green; **5**: black; **6**: orange; **7**: brown; **8**: dark grey; **9**: blue; **10**: red. logP values were calculated by the Instant JChem software (ChemAxon Ltd.)